Clutter Suppression via Hankel Rank Reduction for DFrFT-Based Vibrometry Applied to SAR

Francisco Pérez
University of New Mexico

Balu Santhanam
University of New Mexico

Ranlf Dunkel
General Atomics Aeronautical Systems

Majeed M. Hayat
Marquette University, majeed.hayat@marquette.edu

Clutter Suppression via Hankel Rank Reduction for DFrFT-Based Vibrometry Applied to SAR

Francisco Pérez

The Center for High Technology Materials and the Electrical and Computer Engineering Department, The University of New Mexico, Albuquerque, NM, USA

Balu Santhanam

The Center for High Technology Materials and the Electrical and Computer Engineering Department, The University of New Mexico, Albuquerque, NM

Ralf Dunkel

General Atomics Aeronautical Systems, Inc., San Diego, CA, USA

Majeed M. Hayat

The Center for High Technology Materials and the Electrical and Computer Engineering Department, The University of New Mexico, Albuquerque, NM

Abstract:

Hankel rank reduction (HRR) is a method that, by prearranging the data in a Hankel matrix and performing rank reduction via singular value decomposition, suppresses the noise of a time-history vector comprised of the

superposition of a finite number of sinusoids. In this letter, the HRR method is studied for performing clutter suppression in synthetic aperture radar (SAR)-based vibrometry. Specifically, three different applications of the HRR method are presented. First, resembling the SAR slow-time signal model, the HRR method is utilized for separating a chirp signal immersed in a sinusoidal clutter. Second, using simulated airborne SAR data with 10 dB of signal-to-clutter ratio, the HRR method is applied to perform target isolation and to improve the results of an SAR-based vibration estimation algorithm. Finally, the vibrometry approach combined with the HRR method is validated using actual airborne SAR data.

SECTION I. Introduction

The Hankel rank reduction (HRR) method [1]–[2][3] is a method for clutter suppression that has been extensively used in a high-frequency (HF) ground-wave radar [3]–[4][5]. Specifically, the HRR method was developed as a response to the target detection problem in ocean waters, in which the echoes from the HF radar exhibit high levels of ocean clutter [1]–[2][3]. Particularly, the HRR method exploits the fact that the ocean clutter can be modeled as a combination of narrow-band time-varying signals [3], [4]. Therefore, the ocean clutter can be suppressed by performing singular value decomposition (SVD) of a Hankel matrix of time series data [3].

In parallel, in recent works, the discrete fractional Fourier transform (DFrFT) has proved to be an effective remote-sensing tool for vibration estimation of ground targets in the synthetic aperture radar (SAR) images [6]–[7][8][9][10]. The ability to remotely sense structural vibrations of objects, such as bridges, buildings, and vehicles, can bear vital information about the type, operating conditions, and integrity of these objects. The most appealing characteristic of the DFrFT-based vibrometry approach is that it can be used to retrieve the acceleration time history (waveform), in the range direction, of a vibrating object imaged by an SAR. Therefore, this remote vibrometry technique enables the study of any kind of complex vibration, including chirplike and multicomponent vibrations. In order to do this, the vibrating object's phase history signal contained in an SAR image is processed using the DFrFT in a sliding-window fashion. In this way, the object's instantaneous acceleration is estimated by retrieving the parameters of the chirp modulation (micro-Doppler effect) induced by the objects in each window (subaperture) [6]. However, a major limitation of this vibrometry technique is that it performs poorly when either the signal-to-clutter ratio (SCR) or the signal-to-noise ratio (SNR) decreases below 15 dB [8]–[9][10].

In this letter, we combine both the HRR method and the DFrFT to provide an effective tool for vibration estimation in moderate clutter-level environments. We consider as a moderate clutter an environment where the target can still be distinguished from its surroundings, but the clutter content is high enough to corrupt its SAR signal and, therefore, affect vibration estimation. Under this assumption, the range line corresponding to the SAR phase history of the vibrating object can be isolated by analyzing the magnitude of the complex SAR image (a large magnitude difference is exhibited between the range line corresponding to the target and the range lines corresponding to its surroundings). Specifically, we exploit the fact that the clutter that surrounds a ground target is mainly static. Hence, it naturally complies with the assumptions made in the HRR framework for ocean clutter suppression.

There are several models that have been reported for representing the clutter in SAR images [11]. Generally speaking, these can be classified as parametric or nonparametric models, which can be generated by a speckle model, a product model, or by empirical distributions [11]. In this letter, we limit our study to three specific cases of clutter. First, we analyze the performance of the HRR technique when a simple chirp signal is contaminated with a narrow-band multicomponent sinusoidal clutter. This emulates the type of clutter that static scatterers produce in the SAR signal model (4). Second, in order to emulate the speckle of a ground field, we synthesize an SAR image using (4)with spatially distributed-gamma clutter, and we compare the

performance of our proposal with the DFrFT approach alone. Finally, we use actual airborne SAR data of a vibrating target immersed in a desert clutter to demonstrate the efficacy of the proposed approach.

SECTION II. Hankel Rank Reduction Method

Let $s[n]$, $n = 1, \ldots, N$ be a sampled signal composed of m superimposed sinusoids, whose instantaneous frequencies vary slowly with time. Then, the Hankel matrix of size $(N - L + 1) \times L$ of the time series $s[n]$ can be written as

$$\mathbf{H} = \begin{pmatrix} s[1] & s[2] & \cdots & s[L] \\ s[2] & s[3] & \cdots & s[L+1] \\ \vdots & \vdots & \ddots & \vdots \\ s[N-L+1] & s[N-L+1] & \cdots & s[N] \end{pmatrix} \quad (1)$$

where $L \ll N$ and L is of order $3m$. It has been demonstrated that when the instantaneous frequencies of the sinusoids do not vary significantly over L time steps, the rank of $\mathbf{H}$ will be close to $2m$ [1]. On the other hand, if the instantaneous frequencies are strongly time-varying, $\mathbf{H}$ will be full rank. By means of SVD, the Hankel matrix $\mathbf{H}$ can be expressed as

$$\mathbf{H} = \mathbf{USV}^T = \sum_{j=1}^{P} \sigma_j \mathbf{u}_j \mathbf{v}_j^T \quad (2)$$

where $\mathbf{S} = \text{diag}[\sigma_1, \ldots, \sigma_P]$ and $\sigma_1, \ldots, \sigma_P$ are the singular values of $\mathbf{H}$ in the decreasing order of magnitude, and $\mathbf{U}$ and $\mathbf{V}$ are matrices containing the left- and right-singular vectors, $\mathbf{u}_j$ and $\mathbf{v}_j$, $j = 1, \ldots, P$, respectively. If the instantaneous frequencies of the sinusoids do not present significant variations and if the intensity of the noise is moderate or low, then the most of the power of the signal $s[n]$ will be concentrated in the largest K singular values. Then, the $P - K$ smallest singular values can be neglected and $\mathbf{H}$ can be approximated by

$$\overset{\sim}{\mathsf{H}} = \mathbf{U}_1 \mathbf{S}_1 \mathbf{V}_1^T = \sum_{j=1}^{K} \sigma_j \mathbf{u}_j \mathbf{v}_j^T . \quad (3)$$

Since $\overset{\sim}{\mathsf{H}}$ contains an ordered time structure, similar to that of $\mathbf{H}$ in (1), then an approximation of $s[n]$ (after rank reduction) can be constructed by concatenating the first row with the last column of H~ . In this way, for cases in which the true signal $s[n]$ is contaminated with additive clutter and noise, one can recover a cleaner version of $s[n]$ whenever the singular values of these perturbations have a magnitude less than the largest K singular values of $s[n]$ [1]–[2][3][4] [5].

SECTION III. SAR Signal Model

Let σi be the magnitude of the complex reflectivity of the i th scatterer. Let $r_i[n]$ be the projection of the vibration displacement on the line of sight from the scatterer to the airborne SAR sensor. The range-compressed phase history signal collected by the radar at a given range line [6] can be written as

$$x[n] = \sum_i \sigma_i[n] \exp\left(j\left[\phi_i + y_i f_y n - \frac{4\pi f_c}{c} r_i[n]\right]\right) + \omega[n] \quad (4)$$

where y_i is the cross-range position of the i th scatterer, f_y is an imaging factor, f_c is the carrier frequency, c is the propagation speed of the pulse, and ϕ_i is a constant phase term. For a static scatterer, the term $r_i[n]$ is constant [6]. This model corresponds to the slow-time signal or demodulated pulse, after applying polar-to-rectangular resampling, correcting for cell migration, and applying autofocus. The two assumptions of this model are that the change of an aspect angle in the SAR flight geometry is considered small, and that the phase modulation induced by a time-varying term y_i can be neglected, since, generally, the distance from the patch center to the midaperture is in the order of tens of kilometers. This model is useful for representing the radar return of any scatterer in the scene, including clutter and vibrating objects. However, it makes difficult the task of estimating the vibration waveform of an object, since vibrating objects are usually surrounded by other static objects that produce a sinusoidal clutter with spatial-dependent frequencies. Instead, the DFrFT is applied for estimating the chirp rate of a second-order Taylor approximation of (4) for a point target [6]. Let $r_d[m]$, $v_d[m]$, and $a_d[m]$ be the position, speed, and acceleration of the vibrating target, respectively. Let f_{prf} be the pulse repetition frequency of the SAR and consider a subaperture of N_w samples. Then, in [6], the SAR phase history of a vibrating point target can be expressed as

$$x[n] \approx \sigma \exp(j[\phi - \frac{4\pi f_c}{c} r_d[m] + \left(yf_y - \frac{4\pi f_c}{cf_{\text{prf}}} v_d[m]\right) n$$
$$- \frac{2\pi f_c}{cf_{\text{prf}}^2} a_d[m]n^2]) + \omega[n] \qquad (5)$$
$$m \leq n < m + N_w.$$

In this manner, the vibration waveform can be estimated from (5) by retrieving the chirp parameter $2\pi f_c a_d[m]/(cf_{\text{prf}}^2)$ using a sliding-window approach and assuming $a_d[m]$ to be constant in each window N_w . However, since (5) does not account for the return of static scatterers (clutter) as (4), then the performance of the DFrFT-vibrometry technique becomes susceptible to the clutter that surrounds the vibrating object.

SECTION IV. Applications

A. Chirp Signal and Sinusoidal Clutter

First, we consider the case in which the HRR method is applied to isolate a linear chirp signal, $s[n]$, from the sinusoidal clutter, $c[n]$. This is particularly interesting, because normally in airborne SAR, the signal of interest (SOI) for vibrometry is a linear chirp (produced by the vibrating object) and the surrounding objects act as the sinusoidal clutter. For this experiment, the SOI was a complex-linear chirp of amplitude 1, 0 phase, and frequency ranging from 5 to 10 Hz. The additive sinusoidal clutter was generated as

$$c[n] = \frac{1}{4} \sum_{f=4}^{11} \exp(j2\pi fn + \phi), \phi \sim U[-\pi, \pi]. \text{ (6)}$$

The signals were generated for 2 s at a sampling rate of 2 kHz. The clutter parameters used in (6) were intentionally chosen to interfere with the frequency range of the chirp signal. The HRR method was applied using a Hankel matrix of order 128 and preserving the two most significant singular values. As can be observed in Fig. 1(a) and (b), the HRR method is capable of isolating the chirp signal from the sinusoidal clutter with the similar spectral content. The appropriate number of singular values for the reconstruction was selected by analyzing the singular value spectrum obtained via SVD [see Fig. 1(c)]. When the SCR is known, the following heuristics can be used to determine the approach to follow for recovering the SOI. For the case in which the SCR

is moderate or high, the most significant singular values are likely to correspond to the SOI, and a reliable estimation of the latter can be obtained by disregarding the least significant singular values. Otherwise, when the SCR is low, the most significant singular values are more likely to correspond to the clutter subspace, and clutter reconstruction may be more reliable than signal reconstruction. In this case, an estimation of the SOI can be obtained by subtracting the estimated clutter from the signal. Also, it must be noted that the transition region in the singular value spectrum (transition from the singular values of the signal to those of the clutter) depends on the order of the Hankel matrix employed, as can be seen when comparing the spectrum of a matrix of order 128 [see Fig. 1(c)] and the spectrum of a matrix of order 512 [see Fig. 1(d)]. Therefore, this also determines the number of singular values to preserve.
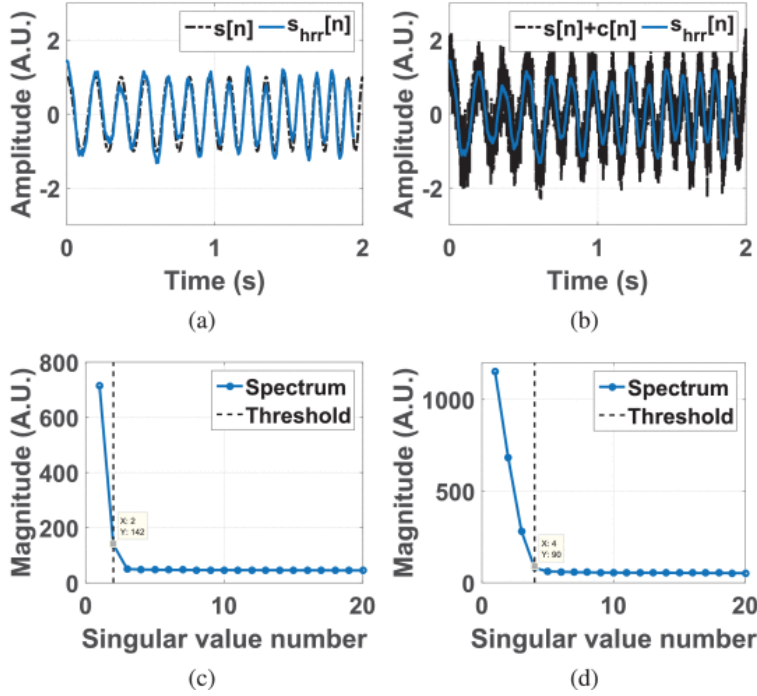

Fig. 1. Results of applying the HRR method on the resulting signal $s[n] + c[n]$. (a) Comparison of $s[n]$ with its estimation via HRR, $s_{\mathrm{hrr}}[n]$ (real part displayed). (b) Comparison of $s[n] + c[n]$ with $s_{\mathrm{hrr}}[n]$ (real part displayed). (c) Singular value spectrum using a Hankel matrix of order 128 of $s[n] + c[n]$. (d) Singular value spectrum using a Hankel matrix of order 512 of $s[n] + c[n]$.

B. Application of HRR on Simulated SAR Data

As a second application, the capability of the HRR method for removing the clutter of moderate level from simulated SAR data is studied. The SAR system parameters used in this simulation experiment are listed in Table I. The SAR data are synthesized using a point target that vibrates at 5 Hz with an amplitude of 1 cm as an element of study (i.e., 5-Hz sinusoidal acceleration of 9.86 m/s²). The SAR signal model utilized for this experiment is (4). On top of the simulated SAR image, spatially distributed-gamma clutter is added at an SCR of 10 dB, and white noise is added at an SNR of 30 dB. The SCR and SNR values are selected in accordance with previous studies that have shown that the standard DFrFT-based vibrometry technique performs poorly for SCR ≤ 15 dB while the SNR is high (SNR ≥ 30 dB) [8]–[9][10]. Once the simulated SAR image is formed, the HRR method is applied to the slow-time data of the complex-SAR image, considering a matrix order of 128 samples, and conserving the 12 most significant singular values for reconstructing the Hankel matrix.

TABLE I SAR System Parameters Used in the Simulation

Parameter	Quantity

Pixel dimension	$0.25 \times 0.25 \text{m}^2$
Nominal resolution	$0.3 \times 0.3 \text{m}^2$
Carrier frequency	Jc= 16GHz
Sent pulse bandwidth	Jo= 454MHz
Pulse duration	$tc = 2 \times 1\text{-}0^4$ s
Length of the synthetic aperture	L = 284m
Plane velocity	Va = 250m/s
Sampling frequency	2.560MHz
Pulse repet iti o n frequency *(fprf)*	450Hz
SNR	30dB
SCR	lOdB

Parameter	Quantity
Pixel dimension	$0.25 \times 0.25\text{m}^2$
Nominal resolution	$0.3 \times 0.3\text{m}^2$
Carrier frequency	$f_c = 16\text{GHz}$
Sent pulse bandwidth	$f_0 = 454\text{MHz}$
Pulse duration	$t_c = 2 \times 10^{-4}\text{s}$
Length of the synthetic aperture	$L = 284\text{m}$
Plane velocity	$V_a = 250\text{m/s}$
Sampling frequency	2.560MHz
Pulse repetition frequency (f_{prf})	450Hz
SNR	30dB
SCR	10dB

Fig. 2(a)–(c) and (e) presents a comparison among the original complex SAR image before and after applying the HRR method. As can be observed, the HRR method significantly reduces the amount of clutter present in the complex SAR image. Specifically, the root-mean-square error (RMSE) between the reference [see Fig. 2(e)] and the SAR image before applying the HRR [see Fig. 2(a)] is 27.6, and the RMSE between the reference and the SAR image after applying the HRR [see Fig. 2(c)] is 18.4. This is even more evident when analyzing the resulting range-compressed SOI, as it is shown in Fig. 2(b)–(d) and (f). It can be noted that, after applying the HRR, the shape of the chirp pulse is partially recovered. Particularly, the RMSE between the range-compressed SOI before applying the HRR and the reference [see Fig. 2(b) and (f)] is 1.39×10^{-3}, and the RMSE between the range-compressed SOI after applying the HRR and the reference [see Fig. 2(d) and (f)] is 0.80×10^{-3}. Then, following the DFrFT-based vibrometry algorithm described in [6], the instantaneous acceleration signal can be estimated from the rang-compressed phase history SOI by applying the DFrFT using a sliding-window approach. For this purpose, we employed the recommend DFrFT parameters for the estimation of low-frequency vibrations [6], [8]. Specifically, a sliding window of 40 samples, an upsampling factor of 4, and a zoom-in factor of 4 were employed in the aforementioned algorithm. The results of applying the DFrFT-based vibrometry algorithm are shown in Fig. 3. As can be observed, preprocessing the data with the HRR method allows one to retrieve a significantly less corrupted acceleration signal. In fact, as it is shown in Fig. 3, the dominant frequency component of 5 Hz can clearly be estimated from the magnitude spectrum when applying the HRR method. Specifically, the RMSE between the recovered acceleration signal without using the HRR and the reference [see Fig. 3(a) and (e)] is 3.66, and the RMSE between the recovered acceleration after using the HRR and the reference [see Fig. 3(c) and (e)] is 1.87. These results demonstrate that the HRR method is a useful tool for dealing with scenarios in which the clutter surrounding the vibrating object has a moderate intensity.
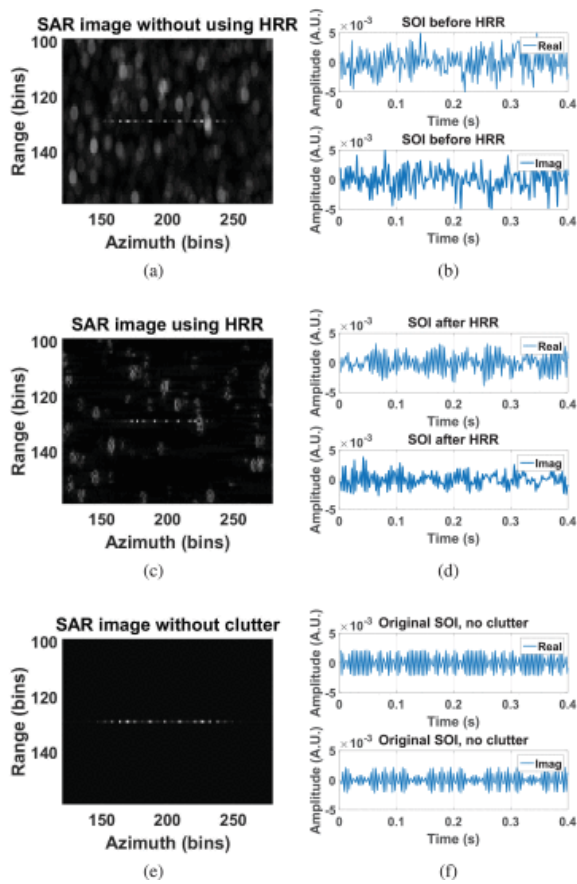
Fig. 2. Result of applying the HRR method on the range-compressed phase history of the simulated data. Magnitude of the SAR image (a) before applying the HRR method, (c) after applying the HRR method, and (e) vibrating target without clutter (reference). Slow-time SOI (b) before applying the HRR method, (d) after the applying HRR method, and (f) vibrating target without clutter (reference).
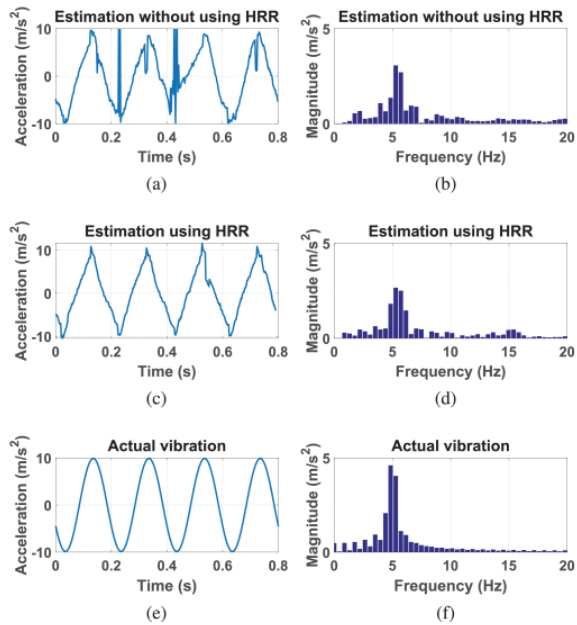

Fig. 3. Acceleration signal of a target vibrating at 5Hz from the simulated SAR data using the DFrFT-based vibrometry approach: (a) Recovered waveform without applying the HRR method, (c) Recovered waveform applying the HRR method, (e) Actual acceleration of the target. Magnitude spectrum of the acceleration signals: (b) Not using the HRR method, (d) Using the HRR method, (f) Spectrum of the actual acceleration of the target.

C. Application of HRR on Real SAR Data

In the last case of study, the HRR method is tested using the real SAR data that were acquired by the Lynx-SAR system of General Atomics Aeronautical Systems at Borrego Springs, CA, USA. The Lynx-SAR system parameters used in the flight test are summarized in Table II. The analyzed vibrating target was a rocking quad corner reflector that vibrated at 3.48 Hz. This target was immersed in a desert-clutter environment (approximately 30 dB of SCR), as shown in Fig. 4(a). Using the same DFrFT approach used in [6], the acceleration signal was retrieved from the range-compressed phase history of the SAR images [see Fig. 4(a) and (b)]. As standard parameters for estimating low-frequency vibrations [6], [8], a sliding window of 40 samples, an upsampling factor of 4, and a zoom-in factor of 4 were employed in the DFrFT algorithm. For this experiment, a Hankel matrix of order 128 was constructed, and only the three most significant singular values were preserved in the rank reduction. The vibrometry results are presented in Fig. 4(b)–(f). As can be observed, when the data are prepossessed using the HRR, the recovered acceleration signal of the target is less noisier than that of the normal case. Furthermore, as can be seen in Fig. 4(b), HRR preprocessing can also be employed to effectively isolate the target from clutter, which is very appealing for target recognition tasks.

TABLE II Lynx-SAR System Parameters

Parameter	Quantity
Pixel dimension	$0.0859 \times 0.0812 \text{m}^2$
Nominal resolution	$0.1016 \times 0.1016111^2$
Carrier frequency	Jc = 15GHz, *Ku* band
Length of the synthetic aperture	L = 176m
Plane velocity	Va = 86.8l m/s
Puls e repetiti on frequency *UvrJ)*	166Hz

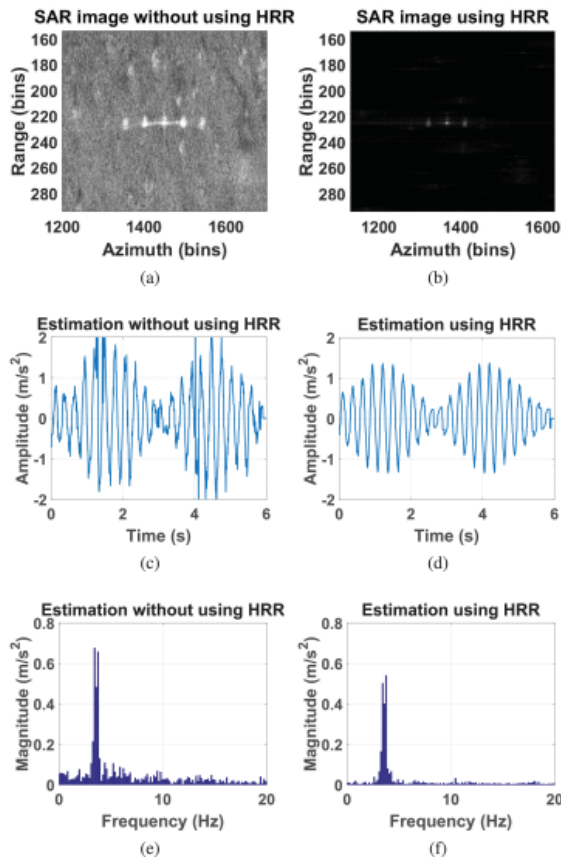| Parameter	Quantity
Pixel dimension	$0.0859 \times 0.0812 \text{m}^2$
Nominal resolution	$0.1016 \times 0.1016 \text{m}^2$
Carrier frequency	$f_c = 15\text{GHz}, K_u$ band
Length of the synthetic aperture	$L = 176\text{m}$
Plane velocity	$V_a = 86.81\text{m/s}$
Pulse repetition frequency (f_{prf})	166Hz

Fig. 4. Results of applying the combined HRR and DFrFT approach on real SAR data containing a target that vibrates at 3.48 Hz. (a) and (b) Magnitude of the complex SAR image captured with the Lynx-SAR system before and after applying the HRR to the slow-time data. (c) and (e) Recovered acceleration signal and its respective magnitude spectrum without applying the HRR. (d) and (f) Recovered acceleration signal and its respective magnitude spectrum when processing the data with the HRR method.

SECTION V. Conclusion

In this letter, the HRR method was applied to SAR images and to the DFrFT-based vibrometry approach for performing clutter suppression. The obtained results demonstrate that the HRR method can effectively be exploited for isolating chirp signals from a sinusoidal clutter. Specifically, it is possible to isolate the vibrating targets from clutter when the HRR method is applied to slow-time SAR data. Moreover, when a vibrating target is embedded in a moderate clutter environment, preprocessing the slow-time SAR data with the HRR method improves the quality of the recovered acceleration signal via the DFrFT. Finally, it is important to remark that the order of the Hankel matrix and the number of singular values to preserve depend on the characteristics of the perturbation affecting the SOI. On the one hand, the order of the Hankel matrix is proportional to the extension of the transition region in the singular value spectrum, which may be useful for separating coupled time-domain features between the signal and the clutter. However, as a consequence of increasing the order of the Hankel matrix, a greater number of singular values will be required to properly approximate the SOI. On the other hand, heuristics and prior knowledge of the SCR can be used for determining which subspace is most reliable to be reconstructed. When the SCR is moderate or high, the most significant singular values of an SVD decomposition of a Hankel matrix are highly likely to belong to the SOI. However, in the case when the SCR is low, the most significant singular values are likely to be part of the clutter, and clutter reconstruction may be more reliable than the reconstruction of the SOI. In this case, an estimation of the SOI can be obtained by subtracting the estimated clutter from the contaminated signal.

References

1. C. L. DiMonte, K. S. Arun, "Tracking the frequencies of superimposed time-varying harmonics", *Proc. Int. Conf. Acoust. Speech Signal Process.*, vol. 5, pp. 2539-2542, Apr. 1990.

2. M. W. Y. Poon, "A clutter suppression scheme for high frequenccy (HF) radar", 1991.

3. R. H. Khan, S. Le-Ngoc, "A singular value decomposition (SVD) based method for suppressing ocean clutter in high frequency radar", *IEEE Trans. Signal Process.*, vol. 41, no. 3, pp. 1421-1425, Mar. 1993.

4. R. H. Khan, "Ocean-clutter model for high-frequency radar", *IEEE J. Ocean. Eng.*, vol. 16, no. 2, pp. 181-188, Apr. 1991.

5. R. Khan, D. Power, J. Walsh, "Ocean clutter suppression for an HF ground wave radar", *Proc. IEEE Can. Conf. Elect. Comput. Eng. Eng. Innov. Voyage Discovery*, vol. 2, pp. 512-515, May 1997.

6. Q. Wang et al., "SAR-based vibration estimation using the discrete fractional Fourier transform", *IEEE Trans. Geosci. Remote Sens.*, vol. 50, no. 10, pp. 4145-4156, Oct. 2012.

7. J. B. Campbell et al., "SAR-based vibrometry using the fractional Fourier transform", *Proc. SPIE*, vol. 9461, pp. 94610O-1-94610O-11, May 2015.

8. F. Pérez et al., "Exploiting synthetic aperture radar imagery for retrieving vibration signatures of concealed machinery", *Proc. SPIE*, vol. 9829, pp. 982903-1-982903-12, May 2016.

9. Q. Wang, B. Santhanam, M. Pepin, M. M. Hayat, "Performance analysis on synthetic aperture radar-based vibration estimation in clutter", *Proc. Conf. Rec. 46th Asilomar Conf. Signals Syst. Comput. (ASILOMAR)*, pp. 217-221, Nov. 2012.

10. Q. Wang et al., "Reduction of vibration-induced artifacts in synthetic aperture radar imagery", *IEEE Trans. Geosci. Remote Sens.*, vol. 52, no. 6, pp. 3063-3073, Jun. 2014.

11. G. Gao, "Statistical modeling of SAR images: A survey", *Sensors*, vol. 10, no. 1, pp. 775-795, 2010, [online] Available: http://www.mdpi.com/1424-8220/10/1/775.